Dual-Mode Microwave System to Enhance Early Detection of Cancer

KENNETH L. CARR, MEMBER, IEEE, ANAS MORSI EL-MAHDI, AND JAMES SHAEFFER

Abstract—**A dual-mode microwave system has been developed that will permit early detection of cancer. The system combines the use of the passive microwave radiometer [1]–[3] with an active transmitter. The active transmitter will provide localized heating to enhance early detection by taking advantage of the differential heating (i.e., tumor temperature with respect to surrounding tissue) associated with thermal characteristics of tumors.**

Introduction

IT IS WELL KNOWN that a carcinoma, or malignant tumor, is normally hotter than the surrounding tissue and that, from "black-body" theory, any perfectly absorbing body emits radiation at all frequencies in accordance with Planck's radiation law. The distribution of radiation is a function of both the temperature and the wavelength, or frequency. It should be noted that as the temperature of the body increases, the density of the radiation or emission at all frequencies also increases. From this viewpoint, infrared thermography, or radiometry, would appear effective; however, transmission losses increase with increasing frequency. Although the highest values of emission occur at the infrared region, an appreciable level occurs at the microwave region.

It is further known [4] that the tumor tissue will die at temperatures above 42°C, and it has been reported [5] that tumor temperatures of greater than 45°C can be held with adjacent normal tissue remaining at or near normal temperature.

The amount of microwave energy needed to provide localized heating is surprisingly low. If we neglect transmission losses and assume that tumor tissue has high water content, similar to that of muscle tissue, and further note that due to vascular insufficiency the tumor will retain and not readily dissipate the absorbed heat, then the amount of power required to elevate the temperature of a tumor 2 cm in diameter, 5° in 1 min, is less than 1.5 W. This can be shown as follows:

$$\text{Quantity of heat, } Q = MC\Delta t, \text{ calories} \tag{1}$$

where mass, M = volume × specific gravity; specific gravity

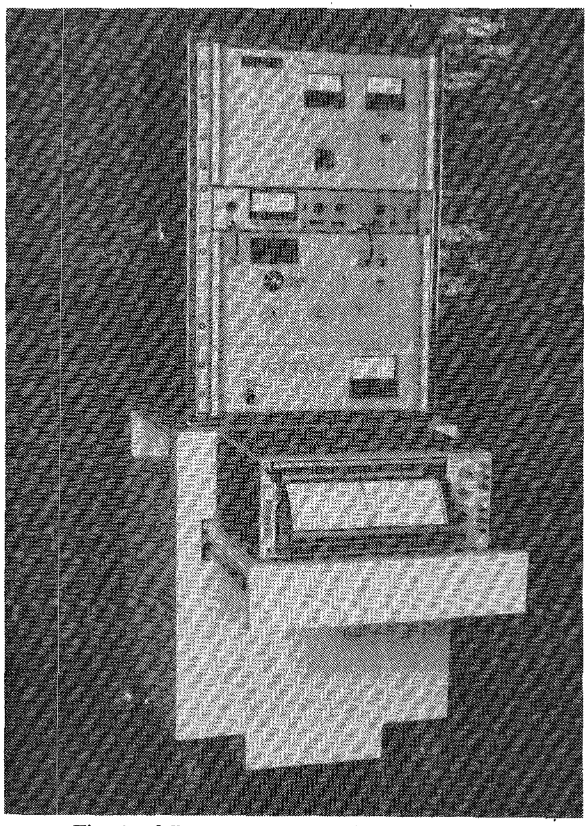

Fig. 1. Microwave system—drawer extended.

of water is 1 g/cm^3; specific heat, °C, is 1 calorie/g·°C; and change in temperature, $\Delta T_r = 5$°C.

The energy Q required to elevate the temperature of the tumor 5°C is 20.95 cal. The power P, therefore, to effect this change in 1 min will be

$$P = \frac{4.18Q}{t}, \quad \text{or } 1.46 \text{ W} \tag{2}$$

where 1 cal = 4.18 J and 1 W = 1 J/s. This calculation assumes that all the heat is transferred to the tumor and the tumor, in turn, does not dissipate this heat. Obviously, if the tumor is near the surface, the actual power required will approximate the calculated value, whereas with a deep tumor transmission losses, scattering, etc., will necessitate additional transmitter power.

This paper describes the design approach taken in the development of the microwave system, shown in Fig. 1, to diagnose and treat cancer using noninvasive techniques. A sensitive passive microwave radiometer specifically de-

Manuscript received September 10, 1980; revised October 24, 1980. This work was supported in part by the National Aeronautics and Space Administration, Langley Research Center, Hampton, VA, under Contract NAS1-15393.

K. L. Carr is with Microwave Associates, Inc., Burlington, MA 01803.
A. M. El-Mahdi and J. Shaeffer are with the Department of Radiation Oncology and Biophysics, Eastern Virginia Medical School, Norfolk, VA 23507.

signed to sense subsurface temperatures is coupled with a solid-state transmitter to provide localized heating of subsurface tissue, thereby taking advantage of the differential heating due to vascular insufficiency associated with the thermal characteristics of tumors to highlight and enhance early detection of cancer.

Design of Microwave System

The system is totally battery operated, allowing approximately 8 h of continuous service prior to recharging. A battery-operated system totally eliminates possible problems associated with line transients, pickup, etc. The portable microwave system is contained in a standard 19-in relay cabinet containing four drawers. The individual drawers are, in essence, totally enclosed housings to minimize interaction—particularly between the sensitive radiometer and the transmitter. The entire cabinet is, in turn, mounted on a movable cabinet as shown in Fig. 1.

The selection of both the radiometer and the transmitter frequencies was based upon several factors:

1) emissivity, which increases with increasing frequency;
2) spatial resolution, which increases with increasing frequency;
3) microwave transmission characteristics (microwave transmission losses generally increase with increasing frequency); and
4) microwave interference.

Based upon the above factors, the frequency chosen for the microwave radiometer was 4.7 GHz which is far removed from the microwave heating frequency of 1.6 GHz.

The microwave radiometer is of the common load comparison, or Dicke, configuration. This configuration greatly reduces the effects of short-term gain fluctuations on the radiometer. The receiver input is switched at a constant rate between the antenna and a constant temperature reference load. The switched, or modulated, RF signal is, therefore, inserted at a point prior to RF amplification and as close to the antenna as possible. In turn, it is then amplified and coherently detected. The final output is now proportional to the temperature difference between the antenna and the reference load. If a second switch ($SW1$ of Fig. 2) is added, the reference load can now be compared with the base load rather than the antenna. If the base load is equal in temperature to the reference load, the dc output of the radiometer will be zero; i.e., a null will be achieved.

In the case where long integration times are involved, long-term gain variations in the receiver must be considered. The long-term, or slow, gain variations can degrade the minimum detectable temperature sensitivity (ΔT) in accordance with the following expression:

$$\Delta T \begin{pmatrix}\text{variation due to} \\ \text{long-term gain change}\end{pmatrix} = \frac{\Delta G}{G} |T_1 - T_2 BV, \text{K} \quad (3)$$

where ΔG is the receiver gain change, G is the nominal receiver gain, T_1 is the temperature of reference load, in kelvins, T_2 is the temperature of base load or antenna, in kelvins (function of calibration switch position).

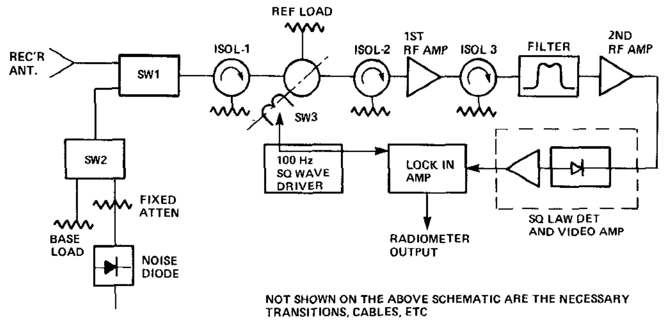

Fig. 2. Microwave radiometer schematic.

Obviously, if T_1 approaches T_2, the effect of long-term receiver gain variations becomes negligible. It becomes advantageous, therefore, to maintain the temperature of both the base load and the reference load approximately equal to the temperature of the antenna.

The radiometer design employs a low-noise RF amplifier in conjunction with a simple single-ended square-law detector rather than the common superheterodyne configuration involving a local oscillator and IF amplifier, thereby minimizing the potential drift and noise associated with this approach.

Fig. 2 represents the simplified block diagram of the radiometer. The calibration switch, $SW1$, is a solenoid-operated mechanical single-pole double-throw switch used to disconnect the antenna and, in turn, to connect the comparison base load. The base load is maintained at a temperature close to that of the reference load. The mechanical switch possesses an isolation of greater than 60 dB with a corresponding insertion loss of less than 0.1 dB. A similar switch, $SW2$, is used in the calibrate path. Its function is to disconnect the base load and to insert a calibrated noise source.

As shown in Fig. 2, there are three ferrite isolators used in the receive path. The first isolator, located between the calibration switch and the Dicke switch, is used to terminate the output of the reference load when the Dicke switch is in the low-loss state. In this state, the reference load is circulated in the direction of the antenna which, in this case, is the ferrite isolator. The second isolator, which is located between the Dicke switch and the first-stage RF amplifier, maintains a constant load match to the amplifier. Any reflections from the RF amplifier would, therefore, be terminated in the isolater. A third isolator is located between the bandpass filter and the output of the first RF amplifier. The purpose of this particular isolator is to present a matched input to the bandpass filter.

A switchable ferrite circulator, $SW3$, has been developed to perform the load comparison or Dicke switch function. The ferrite switch is preferred to the semiconductor approach primarily in view of the lower insertion loss, typically less than 0.25 dB, and elimination of noise generated by the semiconductor junction over and above the measured insertion loss. Briefly, the device is a switchable ferrite junction circulator utilizing the remnant or latching characteristics of the ferrite material. The latching ferrite switch has been constructed in waveguide having a single ferrite element contained within the microwave circuit. The insertion loss was measured and found to be less than 0.25 dB, having isolation in excess of 20 dB.

The RF amplifier is a four-stage FET device constructed in microstrip with integrated biasing circuitry. The noise figure of the first RF amplifier is 2.2 dB with a gain of 35 dB. The second RF amplifier has a noise figure of 2.6 dB with an associated gain of 33 dB. In both instances, the noise figure includes the input ferrite isolator as shown in Fig. 2. With the input and output VSWR at less than 1.5:1, the gain compression at signal levels of between -55 to -10 dBm was less than 0.1 dB.

The bandwidth of the microwave radiometer is basically determined by the bandpass characteristics of the filter. The filter is located after the first RF amplifier to minimize the impact of the insertion loss on the overall system performance. The filter characteristics were chosen to minimize possible interference due to nearby microwave communications or radar bands. The printed, eight-section, bandpass filter is constructed in stripline. The bandwidth is approximately 500 MHz centered at 4.7 GHz. The insertion loss in the passband is less than 3 dB.

The lock-in amplifier enables the accurate measurement of signals contaminated by broad-band noise, power-line pickup, frequency drift, or other sources of interference. It does this by means of an extremely narrow-band detector which has the center of its passband locked to the frequency of the signal to be measured. Because of the frequency lock and the narrow bandwidth, large improvements in signal-to-noise ratio can be achieved. This allows the signal of interest to be accurately measured, even in situations where it is completely masked by noise. In addition, the lock-in amplifier provides the synchronous function associated with the Dicke switch; i.e., the unit supplies the 100-Hz reference clock frequency to drive the ferrite switch driver.

The minimum detectable temperature sensitivity ΔT was well within the desired 0.1°C. The minimum detectable temperature sensitivity ΔT is expressed as follows:

$$\Delta T = \frac{k\left[(FL-1)T_1 + T_2\right]}{\sqrt{B\tau}}, \text{ K}. \tag{4}$$

In the case of the Dicke switch employing square-wave modulation, the value of k is 2.0; F is the noise figure (first amplifier stage), which in our case is 2.2 dB (1.66 ratio); and L is the input losses, expressed as a power ratio. The total loss is 2.0 dB (1.58 ratio).

The effective noise figure FL is, therefore, 2.2+2, or 4.2, which represents a power ratio of 2.63. T_1 is the ambient radiometer temperature (microwave portion); namely, 290 K; T_2 is the source temperature (i.e., temperature seen by antenna), namely 310 K; B is the receiver bandwidth (i.e., the 3-dB bandwidth of the bandpass filter following the first RF amplifier); namely, 500 MHz; and τ is the radiometer output time constant, in seconds.

Utilizing a 3-s time constant, we obtain a minimum detectable temperature sensitivity of

$$\Delta T = \frac{2\left[(2.63-1)290+310\right]}{\sqrt{500\times 10^6 \times 3}}, \quad \text{or } 0.04 \text{ K rms}. \tag{5}$$

Increasing the time constant τ to 10 s results in a ΔT of 0.02 K. Similarly, reducing the time constant to 1 s will result in a ΔT of 0.07 K. The calculated temperature sensitivities are well within our design goal of 0.1°C, as were the actual results.

Microwave Transmitter

The microwave transmitter, shown schematically in Fig. 3, consists of a 1.6-GHz 30-W solid-state source followed by a low-pass filter and microwave reflectometer. Sufficient filtering has been provided through the use of two low-pass filters in series providing 120 dB of attenuation at the third harmonic.

The third harmonic of the 1.6-GHz source is 4.8 GHz which is well within the radiometer passband. The reflectometer, in turn, allows determination of both the reflected and incident power levels. The output power level is electronically adjustable from 0 to 25 W measured at the output of the L-band antenna and, therefore, includes all microwave-circuit and coaxial-cable losses.

Dual-Mode Applicator

It has been determined by Guy [6] that the optimum aperture size to achieve effective coupling of microwave energy associated with layered biological tissue is the simple TE_{10} mode aperture in direct contact with the radiated, or emitting, surface. A normal waveguide transition at L-band corresponding to WR-510 would be 5.10 in (12.95 cm)$\times$2.55 in (6.48 cm). To reduce the physical size of this aperture, single-ridged waveguide was employed since the use of ridged waveguide lowers the frequency at which cutoff will occur. To further reduce the overall size of the aperture, dielectric loading was used.

The dimensions of the ridged portion of the L-band ridged waveguide were selected to allow propagation of the higher frequency associated with the C-band radiometer. The plated surface of the dielectric-loaded C-band waveguide, therefore, formed the single ridge of the L-band waveguide as shown in Fig. 4. The dielectric material used is aluminum oxide having a dielectric constant ϵ_r of 9.8. The C-band aperture dimensions are 0.92 cm$\times$1.83 cm. The overall dimension of the L-band waveguide is 3.66 cm$\times$1.83 cm.

It can be seen in the aforementioned figure that by having the radiometer input contained within the single-ridged waveguide L-band transition, we have placed the point of maximum field of the source of heat in close proximity with that point of thermal detection. The cutoff characteristics of the C-band waveguide have been utilized in addition to other filtering provided, the waveguide forming a high-pass filter to isolate the high-power L-band source from the sensitive radiometer. A heater and proportional thermostat are provided in the dual-mode transition,

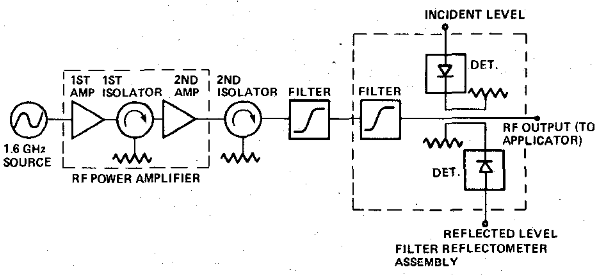

Fig. 3. *L*-band transmitter schematic.

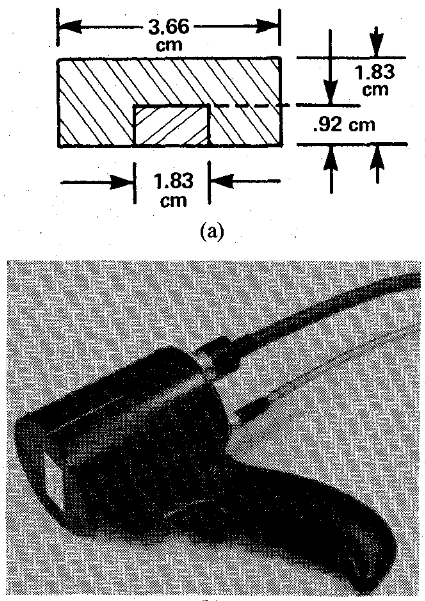

(a)

(b)

Fig. 4. Dual-mode applicator.

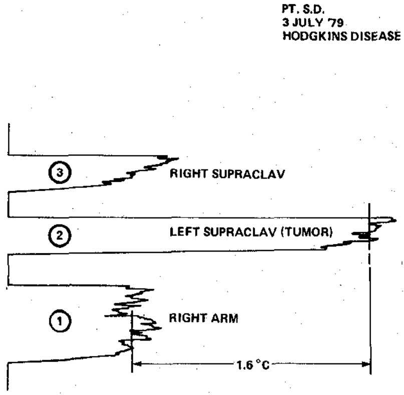

Fig. 5.

TABLE I
PRELIMINARY RESULTS—CLINICAL MICROWAVE THERMOGRAMS

PATIENT	AGE	SEX	DIAGNOSIS	SITE	ΔT
A.B.	58	F	Adenocarcinoma/breast	Right upper outer quadrant	0
A.W.	47	F	Adenocarcinoma/breast	Right upper outer quadrant Left upper inner quadrant	1.2 2.5
D.G.	64	F	Adenocarcinoma/breast	Left upper inner quadrant	1.1
L.C.	73	F	Adenocarcinoma/breast	Right upper outer quadrant	0
B.P.	33	F	Infiltrating carcinoma/ breast	Right breast	1.3
M.C.	34	F	Recurrent breast cancer	Left supraclavicular	0
L.G.	51	F	Recurrent breast cancer	Left anterior chest	3.3
A.M.	57	F	Recurrent breast cancer	Left anterior chest	2.2
R.M.	76	F	Recurrent breast cancer	Right anterior chest	1.1
L.W.	54	F	Recurrent breast cancer	Right anterior chest	1.6
J.D.	75	F	Recurrent breast cancer	Left anterior chest	2.5
L.C.	17	M	Hodgkin's disease	Mediastinum	1.2
S.D.	26	F	Hodgkin's disease	Right supraclavicular	1.6
C.B.	31	M	Hodgkin's disease	Right supraclavicular	0.9
H.E.	70	F	Histiocytic lymphoma	Right leg	0.4*

* Denotes a ΔT in an unresponsive tumor following a course of radiation therapy.

or antenna, to maintain a constant temperature at or very near to that of the temperature of the human body.

It should also be noted that we have taken advantage of the large mismatch associated with the low-impedance ridged waveguide when left open-circuited; i.e., in the atmosphere removed from contact with the human body with its high dielectric constant to which the waveguide is matched. The measured power level in free space measured at a point 1 in from the waveguide opening with the *L*-band power fully on was less than 0.4 mW/cm^2. The safety standard established by ANSI has been 10 mW/cm^2 for electromagnetic radiation, regardless of the frequency; however, this standard is currently under revision to reflect frequency versus power.

CLINICAL DATA

Microwave thermograms were taken on 11 women with biopsy-proven primary or recurrent carcinomas of the breast, as well as 4 patients with lymphoma (see Table I). Temperature differentials (ΔT) consistent with the known tumors were found in 9 of the 12 breast carcinomas and 4 of the lymphomas. It should be noted that one breast cancer patient (A.W.) had bilateral tumors; therefore, there were a total of 12 tumors in the 11 women.

It is noteworthy that although negative results were obtained in 2 breast cancer patients (A.B. and L.C.) for whom xeromammograms were positive, the microwave thermograms were positive in 2 patients (A.W. and D.G.) whose xeromammograms were negative or, at best, inconclusive. It should likewise be mentioned that in the patient with bilateral breast cancer (A.W.), the larger ΔT value of 2.5°C was observed in the smaller lesion (< 10 mm diameter) in the left breast which was not seen in the xeromammograms. The smaller ΔT value of 1.2°C was obtained in the right breast lesion of approximately 2.5-cm diameter, which was seen on xeromammographic (X-ray) studies. Using passive detection only, attempts to locate more deeply seated (lung, esophagus, femur, humerus) malignancies by microwave thermography have all met with failure.

Fig. 5 is a typical scan taken from patient S.D. prior to her course of radiation therapy. Note that a ΔT of 1.6°C was found in her left supraclavicular region. Two months later, following a course of radiation therapy (4000 rads), there was complete resolution of the tumor with a concomitant reduction in the ΔT (Fig. 6). Likewise, there was an increase in ΔT in one patient (R.M.) whose tumor did not respond to radiation therapy. Thus microwave thermogra-

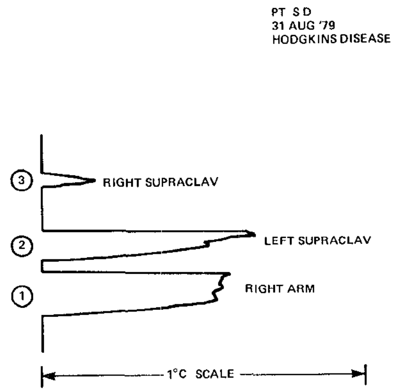

Fig. 6.

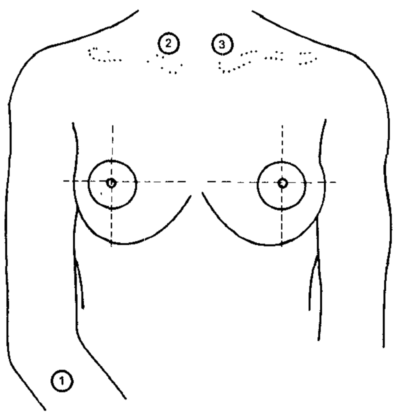

Fig. 7. Note: The encircled numbers correspond to the sensor position of Figs. 5 and 6.

phy may have some potential in assessing the effectiveness of various therapeutic modalities.

Preliminary data using the VX2 carcinoma growing subcutaneously in the ear of a New Zealand white rabbit have demonstrated the feasibility of using heat to enhance the microwave thermographic detection capability of the unit. Under ambient conditions, the ΔT of the VX2 tumor was approximately 1.4°C. This value was increased to values of 1.8–1.9°C 15 to 20 min following heating with the built-in 1.6-GHz transmitter. Further testing of the application of nontherapeutic quantities of heat to enhance tumor ΔT are needed. However, from a theoretical standpoint, if the temperature differential between the tumor and adjacent normal tissue could be increased, one might reasonably expect to be able to detect smaller and/or more deeply seated tumors. When heat is applied to a tumor-bearing volume, the normal tissues have been shown to maintain a much lower temperature than the tumor, presumably because of the greater ability of normal tissues to dissipate excess heat (see Fig. 7).

Insofar as mass screening of breast cancer is concerned, microwave thermography has several distinct advantages over X-ray xeromammography. First, there is no known risk to the patient since the unit is merely monitoring the patient's natural microwave emissions; no harm is done to the patient. Second, there is a possibility (which must be borne out through experimentation) that microwave thermography may be able to detect smaller tumors than can be seen by conventional techniques. This statement has great therapeutic significance since the probability of achieving a cure is inversely related to the size of the tumor at diagnosis.

Acknowledgment

The authors wish to acknowledge the assistance of T. Felderman, M.D., in this investigation.

References

[1] A. H Barrett, P. C. Myers, and M L Sadowsky, "Detection of breast cancer by microwave radiometry," *Radio Sci.*, vol. 12, no. 6(S), p. 167, 1977.

[2] R. A Porter and H H. Miller, "Microwave radiometric detection and location of breast cancer," presented at ELECTRO '78, Boston, MA, May 23–25, 1978

[3] J. Bigu del Blanco and C. Romero-Sierra, "MW radiometry: A new technique to investigate the interaction of MW radiation with living systems," presented at the 27th ACEMB, Philadelphia, PA, Oct 6–10, 1974.

[4] B C. Giovanella, A. C Morgan, J. S. Stehlin, and L. J. William, "Selective lethal effect of supranormal temperatures on mouse sarcoma cells," *Cancer Res.*, vol. 33, p 2568, 1973.

[5] B C. Giovanella, "Correlation of thermosensitivity of cells to their malignant potential," presented at the Conf. on Thermal Characteristics of Tumors: Application in Detection and Treatment, New York Academy of Sciences, Mar. 15, 1979.

[6] A W. Guy, "Electromagnetic fields and relative heating patterns due to a rectangular aperture source in direct contact with bilayered biological tissue," *IEEE Trans. Microwave Theory Tech.*, vol. MTT-19, no. 2, Feb. 1971.

[7] F. K. Storm, W. H. Harrison, R. S. Elliott, C. Hatzitheofilou, and D. L. Morton, "Human hyperthermia therapy: Relation between tumor type and capacity to induce hyperthermia by radiofrequency," *Amer. J. Surgery*, vol. 138, pp. 170–174, 1979b.